# Crystal Structure of Chicken Liver Basic Fatty Acid-Binding Protein Complexed with Cholic Acid[†,‡]

Daniele Nichesola,[§] Massimiliano Perduca,[§] Stefano Capaldi,[§] Maria E. Carrizo,[§] Pier Giorgio Righetti,[||] and Hugo L. Monaco*[,§]

*Laboratorio di Biocristallografía and Laboratorio di Analisi del Proteoma, Dipartimento Scientifico e Tecnologico, Università di Verona, Strada Le Grazie 15, 37134 Verona, Italy*

*Received May 21, 2004; Revised Manuscript Received July 26, 2004*

ABSTRACT: Two paralogous groups of liver fatty acid-binding proteins (FABPs) have been described: the mammalian type liver FABPs and the basic type (Lb-FABPs) characterized in several vertebrates but not in mammals. The two groups have similar sequences and share a highly conserved three-dimensional structure, but their specificity and stoichiometry of binding are different. The crystal structure of chicken Lb-FABP complexed with cholic acid and that of the apoprotein refined to 2.0 Å resolution are presented in this paper. The two forms of the protein crystallize in different space groups, and significant changes are observed between the two conformations. The holoprotein binds two molecules of cholate in the interior cavity, and the contacts observed between the two ligands can help to explain the reason for this stoichiometry of binding. Most of the amino acids involved in ligand binding are conserved in other members of the Lb-FABP family. Since the amino acid sequence of the Lb-FABPs is more similar to that of the bile acid-binding proteins than to that of the L-FABPs, the possibility that the Lb-FABPs might be more appropriately called liver bile acid-binding proteins (L-BABPs) is suggested.

The fatty acid-binding proteins (FABPs)[1] are a superfamily of low-molecular mass (∼15 kDa) molecules that can bind and solubilize fatty acids and other lipophilic ligands (*1*−*6*). Although the specific function of each member of the group has not yet been established, it is generally assumed that it is related to solubilization, storage, and transport of one or more hydrophobic ligands. Characteristic of the family is a common fold in which 10 strands of antiparallel $\beta$-sheet surround the hydrophobic ligand binding site. Two short α-helices, found topologically between the first and second strands, are believed to undergo a conformational change that would create an opening in the otherwise closed $\beta$-barrel and that would allow the ligand to enter or exit the internal cavity (*7*). The family has many members, and more than 15 sequences are known, with the proteins being named according to the organ from which they were originally extracted. There are, however, several cases in which more than one FABP is found in a single type of tissue and others in which the same protein is found in several organs. Although the essential features of the fold are very strictly conserved in all members, the FABPs isolated from different cells can have a very low level of sequence homology, but when the same tissue is considered in different species that can be quite distant in evolution, a much higher degree of sequence similarity, up to 70−80%, is observed.

In the liver, two paralogous groups of fatty acid-binding proteins (FABPs) have been described: liver fatty acid-binding protein (L-FABP) (*8*−*10*) type, extensively characterized in mammals, and liver (basic) fatty acid-binding proteins (Lb-FABP) that have not yet been found in mammalian liver but have been described in several other vertebrates (*11*−*14*). The word "basic" was added to the acronym FABP to name the first member of this family identified in chicken liver, because the protein turned out to have an isoelectric point (pI) of 9.0, and it was known that there was another chicken liver FABP with a different pI and amino acid composition (*11*). The division of the liver FABPs into two subgroups is based on sequence homology but also on the differences observed in their binding properties. The mammalian L-FABPs differ from most other members of the FABP family in that they bind two fatty acid molecules (*9*), whereas the Lb-FABPs have been shown to bind a single fatty acid molecule (*15*, *16*).

Several years ago, we determined the X-ray structure of apo chicken Lb-FABP to 2.7 Å resolution (*17*), but did not refine the model because of the modest amount of diffraction data available at that resolution and also because, at the time, the amino acid sequence of the protein was unknown (*18*). Since then, significantly higher resolution data have been collected and that model has been refined, but up to the time we tested cholate, we had not been able to prepare cocrystals

[†] M.E.C. is the recipient of a fellowship from the Argentine Consejo Nacional de Investigaciones Científicas y Técnicas. This work was supported by a PRIN (Progetto di Ricerca di Interesse Nazionale) grant, "Structural studies on hydrophobic molecule-binding proteins", from the Italian Ministry of the Universities and Scientific Research and by the Italian Space Agency (ASI, Grant I/R/294/02).

[‡] The coordinates of the model and the structure factors of the apoprotein and of the complex with cholate have been deposited in the Protein Data Bank (entries 1TVQ and 1TW4).

* To whom correspondence should be addressed. Phone: 39 045 8027 903. Fax: 39 045 8027 929. E-mail: monaco@sci.univr.it.

[§] Laboratorio di Biocristallografía.

[||] Laboratorio di Analisi del Proteoma.

[1] Abbreviations: BABP, bile acid-binding protein; FABP, fatty acid-binding protein; GT, gastrotropin; I-BABP, ileal bile acid-binding protein; L-FABP, liver fatty acid-binding protein; Lb-FABP, liver basic fatty acid-binding protein; L-BABP, liver bile acid-binding protein; rms, root-mean-square.

10.1021/bi0489661 CCC: $27.50 
Published on Web 10/12/2004

in which the electron density maps of the ligand were sufficiently clear and convincing.

The X-ray structure of the cocrystals of chicken Lb-FABP complexed with cholate, a reasonable endogenous ligand for a liver protein, is presented in this paper, and the model of the holoprotein is compared with that of the apoprotein refined to 2.0 Å resolution. Examination of the sequence similarities between this protein and other lipid-binding proteins shows that its sequence is more similar to that of other bile acid-binding proteins (or gastrotropins) (*19*−*21*). The bile acid-binding proteins are molecules of considerable medical and pharmacological interest since their ligands are produced from cholesterol and they play an essential role in lipid absorption. The best characterized member among them is the ileal bile acid-binding protein (or lipid-binding protein or gastrotropin), and there are several studies using NMR and other structural techniques dealing with its structure and ligand binding properties (*22*−*27*). However, to the best of our knowledge, no X-ray diffraction analysis has been published. We thus believe that the results presented here can also be of interest as a model for binding of cholate to these recognized bile acid transporters and examine the hypothesis that the Lb-FABPs may be more accurately described as bile acid-binding proteins rather than fatty acid-binding proteins.

## MATERIALS AND METHODS

*Protein Purification, Complex Formation, and Crystallization.* The protein was purified by a modification of the method of Scapin et al. (*11*) in which the last preparative isoelectric focusing step was substituted with separation in a multicompartment electrolyzer (*28*). The electrolyzer was assembled with five chambers, delimited by the following membranes: pI 5.0, 7.0, 8.8, and 11.0 (all made to contain 5% T, 4% C polyacrylamide). Endogenous lipids were removed in a lipidex 1000 column. To prepare the complex with the ligand, the apoprotein was diluted to a concentration of 1 mg/mL in 50 mM Tris-HCl buffer (pH 7.5), and 10 times the molar protein concentration of sodium cholate was added to the solution. The solution was stirred overnight at 20 °C before being concentrated under nitrogen pressure to 30 mg/mL.

Crystals of both the apoprotein and the complex were grown under microgravity conditions on the International Space Station during the STS-100/ISS 6A mission. The same crystals could be grown on Earth, but they were smaller and diffracted to a slightly worse resolution. The crystallization experiments were carried out using the growth cell assembly of the new High-Density Protein Crystal Growth System (HDPCG) developed at the University of Alabama at Birmingham (*29*). Forty microliter droplets were prepared by mixing equal volumes of the protein solution and 0.1 M imidazole (pH 7.5) and 20% PEG 6000. The crystallization reservoir contained 550 $\mu$L of the precipitating solution.

*Data Collection, Structure Solution, and Refinement.* The cocrystals of chicken liver basic FABP and cholate are orthorombic, space group $P2_12_12_1$, and unlike the crystals of the apoprotein contain two molecules in the asymmetric unit (see Table 1). Data for both the apoprotein and the cocrystals were collected at the XRD1 beamline of the Elettra synchrotron in Trieste, Italy ($\lambda = 1.00$ Å), at 100 K after a brief soaking in a mixture of 70% mother liquor and 30% glycerol. Two data sets, at high and low resolution, were collected with a Mar CCD detector using the same frozen crystal. The data were indexed, integrated, and reduced using MOSFLM (*30*) and Scala (*31*). The structure of the Lb-FABP−cholate complex was determined using the CCP4 suite of programs for crystallographic computing (*31*). The initial phases were calculated by the molecular replacement method as implemented in AMoRe (*32*), with the coordinates of axolotl Lb-FABP (unpublished) as the search probe. When the rotation function was calculated with the data in the 8.0−3.5 Å resolution range, the three highest peaks had correlation coefficients of 25.4, 18.5, and 18.1. The fourth peak had a correlation coefficient of 17.0. When the translation function was calculated, the first peak gave an unambiguous and convincing answer for the first molecule in the asymmetric unit. The correct solution for the second molecule was not the second but the third peak of the rotation function which was confirmed by examination of the molecular packing in this unit cell. The correlation coefficient of the solution with the two molecules in the asymmetric unit was 39.1% and its *R* factor 48.3%. The model was rigid body refined with the data up to 3.5 Å resolution, moving initially the entire molecule and, in a second stage, the elements of secondary structure using CNS (*33*). After the proper side chains had been introduced, the model was subjected to a series of rounds of positional refinement alternated with manual model revisions with O (*34*) and CNS. During the process of refinement and model building, the quality of the model was controlled with PROCHECK (*35*). Solvent molecules were added to both the models of the apoprotein and the complex with cholate in the final stages of refinement according to hydrogen bond criteria and only if their *B* factors refined to reasonable values and if they improved the $R_{free}$.

Table 1: Data Collection and Refinement Statistics[a]

| | apoprotein | complex with cholic acid |
|---|---|---|
| **Data Collection** | | |
| space group | $P2_12_12_1$ | $P2_12_12_1$ |
| unit cell parameters (Å) | $a = 39.49$, $b = 60.34$, $c = 65.89$ | $a = 60.31$, $b = 63.41$, $c = 77.23$ |
| no. of observed reflections | 60486 | 111640 |
| no. of independent reflections | 11069 | 19076 |
| redundancy | 5.5 | 5.9 |
| $R_{sym}$ (%) | 4.7 (4.7) | 6.3 (10.0) |
| $\langle I/\sigma(I)\rangle$ | 8.8 (12.7) | 5.9 (5.9) |
| overall completeness (%) | 99.3 (100.0) | 97.1 (80.0) |
| **Refinement** | | |
| resolution range (Å) | 30.0−2.00 (2.07−2.00) | 30.0−2.00 (2.07−2.00) |
| no. of reflections in the working set | 9939 (997) | 17063 (402) |
| no. of reflections in the test set | 1096 (102) | 1864 (39) |
| $R_{cryst}$ (%) | 23.3 (23.0) | 21.6 (22.9) |
| $R_{free}$ (%) | 27.0 (29.0) | 25.7 (27.1) |
| no. of protein atoms | 989 | 1978 |
| no. of ligand atoms | 0 | 116 |
| no. of water molecules | 127 | 249 |
| rmsd for bond lengths (Å) | 0.008 | 0.008 |
| rmsd for bond angles (deg) | 1.426 | 1.396 |
| rmsd for dihedrals (deg) | 27.509 | 26.357 |
| rmsd for impropers (deg) | 0.727 | 1.333 |
| average *B* factor (Å$^2$) | 24.81 | 24.27 |
| protein atoms | 23.80 | 23.30 |
| ligand atoms | − | 19.91 |
| solvent atoms | 32.71 | 33.70 |

[a] The values in parentheses refer to the highest-resolution shell: 2.00−2.11 Å for the apoprotein and 2.03−2.14 Å for the holoprotein.

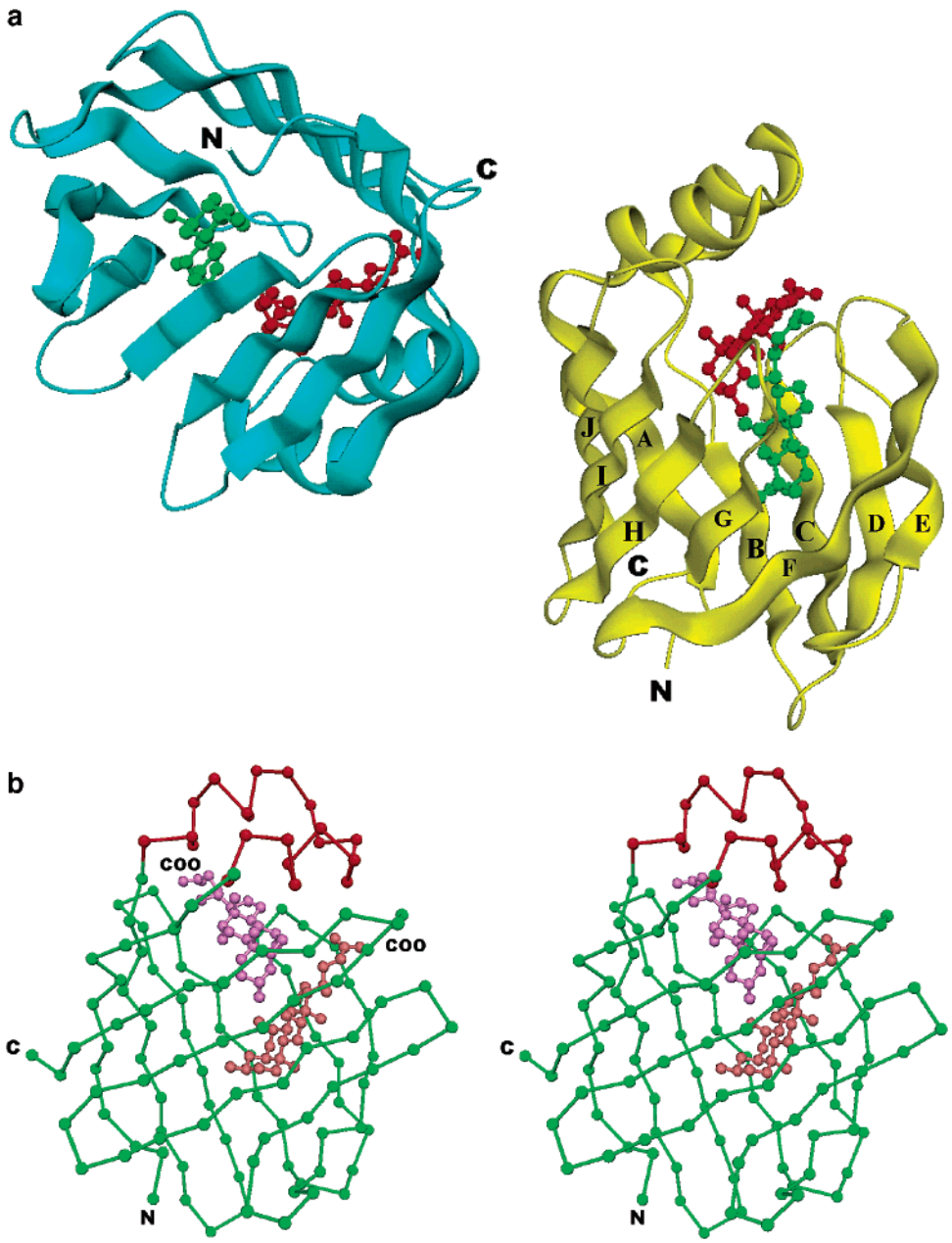


FIGURE 1: Crystal structure of chicken Lb-FABP complexed with cholic acid. (a) Ribbon representation of the two molecules present in the crystallographic asymmetric unit. The elements of secondary structure are labeled in the yellow molecule. (b) Stereoview of the Cα chain trace of one protein chain with the two cholate molecules bound in its interior. This figure was prepared using Dino (http://www.dino3d.org).

## RESULTS AND DISCUSSION

*Refined Structure of the Apoprotein.* The crystal structure of apo chicken Lb-FABP was refined to a resolution of 2.0 Å starting with the model built to fit the electron density map calculated with MIR phases at 2.7 Å resolution (*17*). The final model corresponds to the full-length 125-amino acid chain, 989 protein atoms, and 127 water molecules. The conventional $R$ factor is 23.3% and $R_{free}$, calculated with 10% of the reflections, 27.0% (Table 1). The $R$ factors and rms deviations listed in Table 1 were calculated with CNS (*33*). The stereochemical quality of the protein model was assessed with PROCHECK (*35*). In this model, 92.9% of the residues are in the most favorable region of the Ramachandran plot and the remaining 7.1% in the additionally allowed region. The overall fold consists of the canonical $\beta$-barrel with 10 strands of antiparallel $\beta$-chain and the two α-helices inserted between the first and second strand.

*Structure of Chicken Lb-FABP in Complex with Cholate.* The cocrystals of chicken Lb-FABP and cholic acid belong to a crystal form that is different from that of the apoprotein and contain two molecules in the asymmetric unit. The structure, which was determined by molecular replacement, was refined to a resolution of 2.0 Å without imposing noncrystallographic symmetry. The final model contains 1978 protein atoms, 116 ligand atoms (four cholate molecules), and 249 water molecules. The conventional $R$ factor is 21.6% and $R_{free}$, calculated with 10% of the reflections, 25.7% (Table 1). In this model, 92.4% of the residues are in the most favorable region of the Ramachandran plot and the remaining 7.6% in the additionally allowed region. Figure 1a is a cartoon representation of the two molecules present

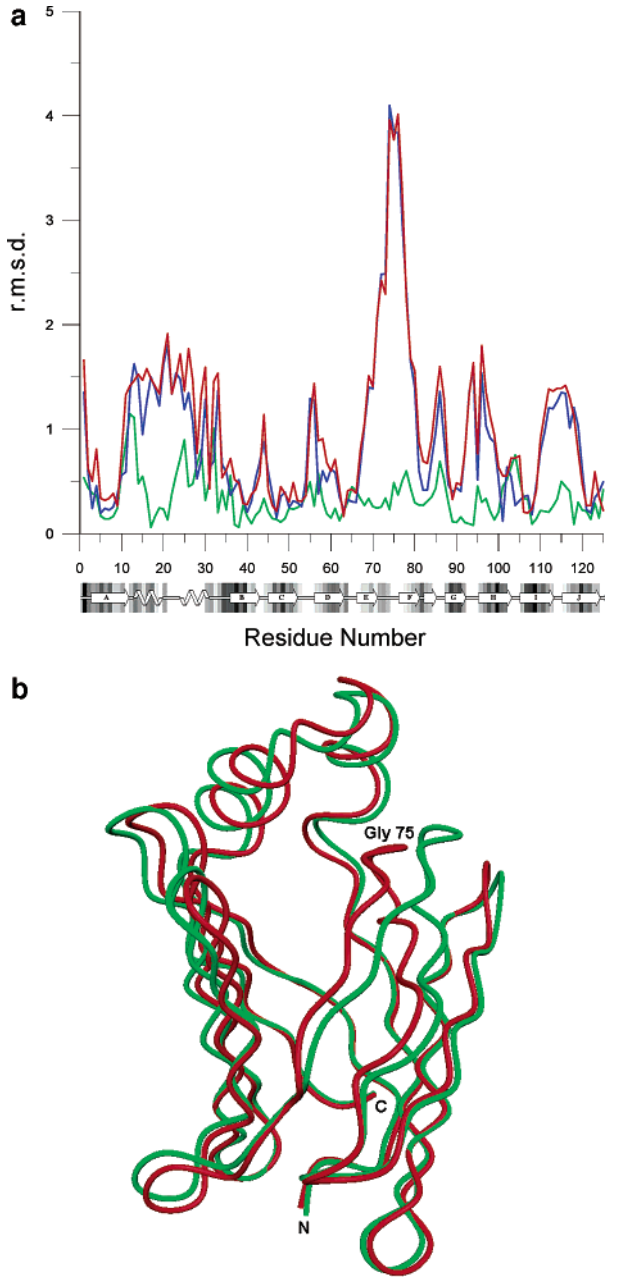


FIGURE 2: Comparison of the apo- and holoprotein models. (a) Values of the rmsd between α-carbon atoms of the apoprotein model and the A chain (blue) and B chain (red) of the cholate complex model and values of the rmsd between α-carbon atoms of the A and B chains of the cholate cocrystal model (green). The strip at the bottom of the figure represents the elements of secondary structure. (b) Models of the apoprotein (red) and holoprotein (green) superimposed using LSQKAB (*36*). Note that the cavity covered by the two helices is more open in the holoprotein. The region where the two polypeptide chains are more distant is the loop connecting strands E and F.

in an asymmetric unit of this crystal form. Figure 1b is a stereodiagram of one of the molecules showing the two cholic acids bound in the interior cavity, while Figure 3a shows the electron density of the two ligands found in the active site of one of the two Lb-FABP molecules.

Using LSQKAB (*36*), the two molecules in the asymmetric unit were superimposed and the distances between equivalent α-carbons were calculated. They are represented in Figure 2a as a function of the amino acid number. The same program was used for an analogous comparison of each molecule in the asymmetric unit of the cocrystals and the model of the apoprotein. These results are also represented in Figure 2a. While no interpretable differences are evident between the two molecules in the asymmetric unit, the differences between each of the two holo molecules and the model of the apoprotein are quite significant and almost identical to each other. In particular, the peak showing the largest deviations in the main chain is in the loop connecting strands E and F and, to a lesser extent, in the region of the two α-helices and other areas evidenced in the figure. Figure 2b shows a holo molecule (green) superimposed with an apo molecule (red). Note that while the regions of the molecule opposite from the cap containing the two helices superimpose quite well, the helices and strands E and F are in a more open conformation in the holoprotein. It is also worth mentioning that the side chains of several amino acids in these areas are involved in ligand binding (see below).

The solvent accessible volumes of the ligand-binding cavity of the two molecules of the holoprotein in the asymmetric unit, calculated with CASTp (*37*), are 627.0 and 627.4 Å$^3$, i.e., virtually identical, but an analogous calculation with another program gives somewhat different results. The same calculation yields a value of 143.7 Å$^3$ for the apoprotein which clearly shows that the conformational change takes place, as expected, with an increase in the volume of the ligand-binding cavity.

We have also used the GRID-docking program (*38*, *39*) to examine the binding of cholate to the two models of chicken Lb-FABP. The result of this analysis is that, while the energetically most favored sites are found on the surface of the apoprotein, the two experimentally determined sites of the holoprotein are correctly predicted as well as two other alternative sites, which are also in the interior of the cavity. This result confirms that the different conformation of the holoprotein is energetically more favored for the binding of the ligand molecules inside the molecular internal cavity.

*Ligand Binding.* The electron density for two cholate ligands is very clear in the two Lb-FABP molecules present in the asymmetric unit so that, in these crystals, this stoichiometry of binding is beyond discussion. As seen in Figure 1a, the two molecules are found in the interior cavity of the protein with no evidence of binding to the surface of Lb-FABP as proposed for rabbit ileal BABP (*24*). This situation is quite different from what we have observed for other ligands such as palmitic or oleic acid, since in those cases the electron densities in the ligand regions of the map were not well ordered (data not shown). A stoichiometry of binding of two bile acid molecules per binding site has also been proposed for the structurally related human ileal BABP (*25*, *27*), but there is currently no X-ray structure of the complex available. Clearly, the dimensions of the central cavity in the holo conformation are sufficient to accommodate the two cholate molecules, and the fact that this protein binds only one fatty acid, while the structurally related mammalian L-FABP binds two (*9*), is more related to side chain position than to cavity size.

Table 2 lists the distances shorter than 3.7 Å between atoms of the two ligand molecules (labeled 130 and 131) present in the central cavity and the side chains of each of the two protein molecules in the asymmetric unit (A and B). Note that the same interactions are found in the two protein molecules and that the values of the distances are

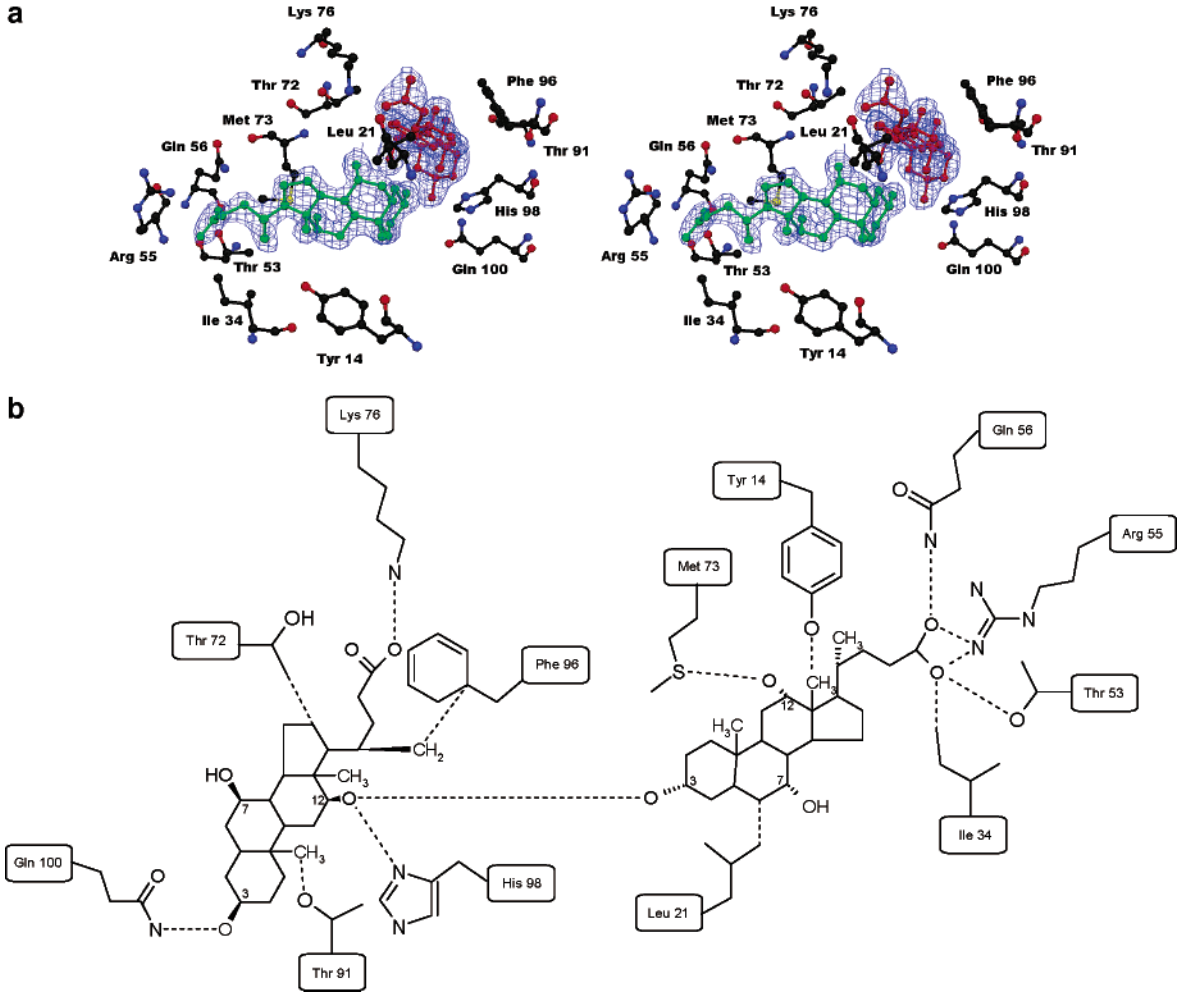


FIGURE 3: Binding of cholate to chicken Lb-FABP. (a) Stereodiagram showing the amino acids that are in closest contact with the two bound ligands listed in Table 2. The $2F_{obs} - F_c$ map was contoured at a 1.5$\sigma$ level. (b) Schematic representation of the interactions shown in panel a.

Table 2: Distances between the Closest FABP Residues and the Cholate Molecules and between the Two Ligands Bound in Each of the Two Binding Sites of the Crystallographic Asymmetric Unit

Main Contacts between the Cholic Acid Molecules and FABP Residues

| cholate molecule | atom | FABP residue | atom | distance (Å) | cholate molecule | atom | FABP residue | atom | distance (Å) |
|---|---|---|---|---|---|---|---|---|---|
| A130 | C18 | Tyr A14 | OH | 3.41 | B130 | C18 | Tyr B14 | OH | 3.55 |
| A130 | C6 | Leu A21 | CD2 | 3.44 | B130 | C6 | Leu B21 | CD2 | 3.63 |
| A130 | O25 | Ile A34 | CD1 | 3.64 | B130 | O25 | Ile B34 | CD1 | 3.29 |
| A130 | O25 | Thr A53 | OG1 | 3.36 | B130 | O25 | Thr B53 | OG1 | 3.68 |
| A130 | O25 | Arg A55 | NH1 | 3.63 | B130 | O25 | Arg B55 | NH1 | 3.39 |
| A130 | O26 | Arg A55 | NH1 | 2.33 | B130 | O26 | Arg B55 | NH1 | 3.48 |
| A130 | O26 | Gln A56 | NE2 | 2.82 | B130 | O26 | Gln B56 | NE2 | 2.78 |
| A130 | O12 | Met A73 | SD | 3.53 | B130 | O12 | Met B73 | SD | 3.23 |
| A131 | C16 | Thr A72 | CG2 | 3.40 | B131 | C16 | Thr B72 | CG2 | 3.35 |
| A131 | O26 | Lys A76 | NZ | 2.94 | B131 | O26 | Lys B76 | NZ | 2.70 |
| A131 | C19 | Thr A91 | OG1 | 3.02 | B131 | C19 | Thr B91 | OG1 | 3.18 |
| A131 | C21 | Phe A96 | CG | 3.52 | B131 | C21 | Phe B96 | CG | 3.49 |
| A131 | O12 | His A98 | ND1 | 2.70 | B131 | O12 | His B98 | ND1 | 2.71 |
| A131 | O3 | Gln A100 | NE2 | 2.77 | B131 | O3 | Gln B100 | NE2 | 2.81 |

Contacts between the Two Pairs of Cholic Acid Molecules

| cholate molecule | atom | cholate molecule | atom | distance (Å) | cholate molecule | atom | cholate molecule | atom | distance (Å) |
|---|---|---|---|---|---|---|---|---|---|
| A130 | C3 | A131 | O12 | 3.48 | B130 | C3 | B131 | O12 | 3.49 |
| A130 | O3 | A131 | O7 | 3.83 | B130 | O3 | B131 | O7 | 3.88 |
| A130 | O3 | A131 | O12 | 2.74 | B130 | O3 | B131 | O12 | 2.73 |
| A130 | O3 | A131 | C14 | 3.68 | B130 | O3 | B131 | C14 | 3.72 |
| A130 | C4 | A131 | O12 | 3.98 | B130 | C4 | B131 | O12 | 3.77 |
| A130 | C4 | A131 | C17 | 3.79 | B130 | C4 | B131 | C17 | 3.93 |

quite similar. Figure 3a is a stereodiagram representing the amino acid side chains in contact with the two cholate molecules, and Figure 3b is a schematic representation of the interactions. Table 2 also lists the distances shorter than 4 Å between the two cholate molecules bound to each of the two protein molecules in the asymmetric unit. Note, in

particular, the distances between O3 of one cholate molecule (molecule 130 in our notation) and O12 of the other, 2.73 and 2.74 Å, and O3 of the same molecule and O7 of the other cholate molecule (molecule 131 in our notation), 3.83 and 3.88 Å. O3 of molecule 131 is in contact with NE2 of Gln 100.

The main hydrophobic contacts observed between the protein and the ligands are with Phe 17, Leu 18, Leu 21, Leu 27, Ile 34, Phe 62, Ile 70, Met 73, Val 82, Phe 96, Ile 111, and Leu 118. Of the two ligand molecules, the one that has more hydrophobic contacts with these amino acids is the molecule we have labeled 130, the reason being that it is buried more deeply in the cavity.

*Cooperativity of Ligand Binding.* The cooperativity of binding of glycocholic acid to human ileal BABP has received considerable attention (*25*, *27*). For this system, it was proposed that it is the hydroxylation pattern of the ligand that governs cooperativity, and two possible mechanisms were suggested to explain it: a conformational change induced in the protein by the binding of the first bile acid molecule and/or the creation of a more favorable surface of interaction for the second ligand because of the presence of the first in the binding cavity (*27*). In the case of chicken Lb-FABP, we have identified important contacts between the two bound cholate molecules in the fully ligated protein (Table 2), but we have also observed a significant conformational change in the transition between the apo and holo forms of the macromolecule, accompanied by an increase in the volume of the ligand binding site. Therefore, although we have no information about the protein conformation with a single cholic acid bound, it would appear that in the case of chicken Lb-FABP, both mechanisms are present.

*Comparison with Other Lipid-Binding Proteins.* Figure 4 compares the amino acid sequence of chicken Lb-FABP with those of four mammalian type L-FABPs, with the four ileal BABPs of the same species, and with chicken L-FABP. The four species (human, rat, mouse, and pig) are those for which the sequences of both the L-FABP and the ileal BABP are currently available. The 10 sequences were aligned using CLUSTAL W (*40*). The identity percentage of each sequence and that of chicken Lb-FABP are given in the column on the right-hand side of the figure. A comparison of the values for each of the four species indicates that chicken Lb-FABP appears to be more similar to the BABPs than to the mammalian type L-FABPs. The last row of each of the two groups of sequences identifies the amino acids that are identical in chicken Lb-FABP and all four sequences in each of the two groups. There are 39 in the case of the L-FABPs and 42 in the case of the BABPs. These observations, added to the results presented here, support the proposal that the main function of the Lb-FABPs is more likely to be binding bile acids and not fatty acids. The fact that this protein also binds fatty acids is not unexpected since a similar lack of specificity has also been observed in other members of the FABP family.

The possibility that the mode of binding of cholic acid to chicken Lb-FABP may be extended to other Lb-FABPs, as well as to the BABPs that have not yet been crystallized in the presence of bile acids, deserves attention.

Di Pietro et al. (*41*) have aligned the 10 available sequences of the Lb-FABPs and identified the residues present in all the members of this family and absent in the

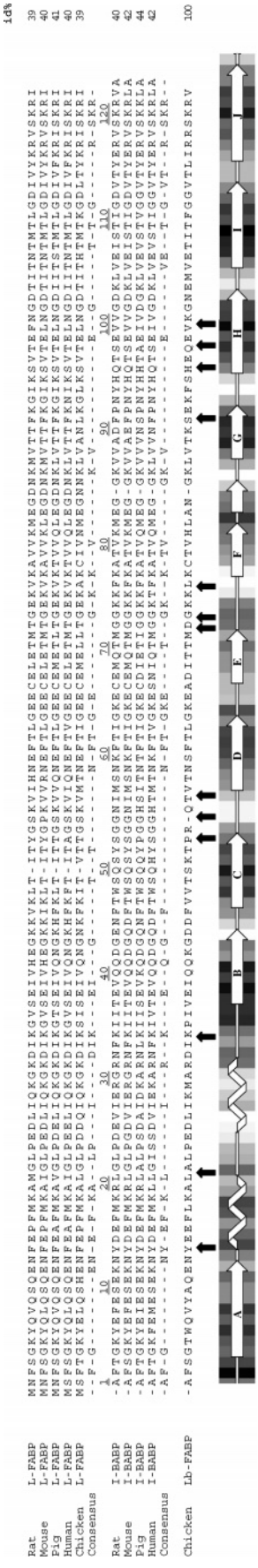


FIGURE 4: Sequence comparison of chicken Lb-FABP and four members of the mammalian type L-FABP family and the ileal BABPs of the same species. The four species are those for which both the L-FABP and BABP sequences are available. The fifth row of the L-FABP group is the chicken L-FABP. The 10 sequences were aligned using CLUSTAL W (*40*). The column on the right-hand side of the figure gives the identity percentage of each sequence and that of chicken Lb-FABP. The last line of each group of sequences has the amino acids identical in all the sequences of the group and in chicken Lb-FABP. The amino acids of chicken Lb-FABP involved in cholate binding are denoted with arrows, while the bottom strip represents the elements of secondary structure of the protein.

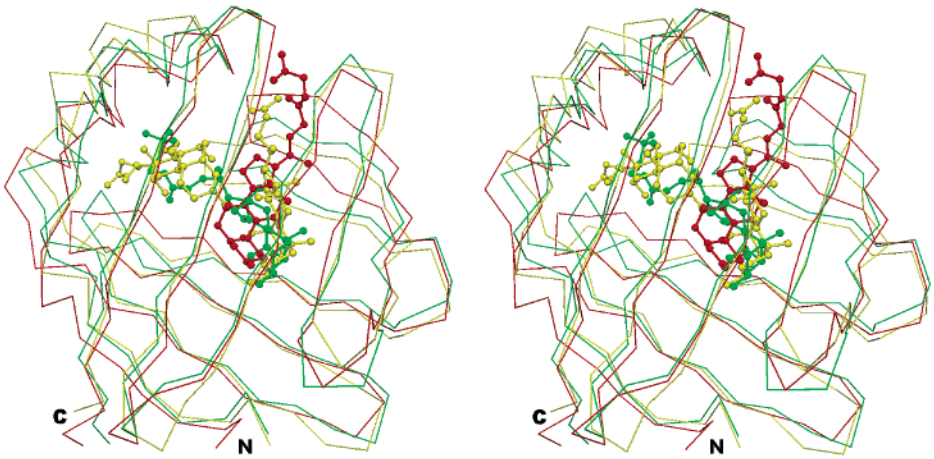


FIGURE 5: Stereodiagram of the two cholate molecules superimposed on the molecules of glycocholate and taurocholate bound to the ileal BABPs. The coordinates of chicken Lb-FABP were superimposed with those of porcine ileal BABP complexed with glycocholate [PDB entry 1EIO (*23*)] and human ileal BABP complexed with taurocholate [PDB entry 1O1V (*26*)] by using LSQKAB (*36*). The coordinates used for both NMR structures were the first sets listed in the PDB files. The two cholate molecules bound to chicken Lb-FABP are represented in yellow, and the glycocholate molecule is red and the taurocholate molecule green.

mammalian L-FABPs. When the residues in contact with the ligands, identified in Table 2, are examined in that alignment, it is found that they are highly conserved with two exceptions: Arg 55, which is a Lys in some cases and a Gln in others but is also a Gly in three species, and Thr 91 which, interestingly enough, is a Cys in the majority of the Lb-FABPs.

The residues of chicken Lb-FABP involved in cholate binding are marked with arrows in Figure 4. Note that Lys 76, which is highly conserved in the ileal BABPs (and also in the Lb-FABPs; see ref *41*), becomes a Glu in all the L-FABPs that are listed. Among the residues identified by Di Pietro et al. as strictly conserved in all the Lb-FABPs and absent in the L-FABPs (*41*), Phe 96, His 98, and Gln 100 are involved in cholate binding.

Using NMR data, two alternative modes of binding for a single molecule of glycocholate and taurocholate to porcine and human ileal BABP, respectively, have been proposed (*23*, *26*). Both are different from either of the two positions that we observe in the crystals for the binding of cholate to chicken Lb-FABP. Using LSQKAB (*36*), we have superimposed these two sets of coordinates [PDB entries 1EIO (*23*) and 1O1V (*26*)] with the coordinates of chicken Lb-FABP and examined the position of the ligands in the three models. Figure 5 is a stereodiagram that shows the three protein structures superimposed and the models of glycocholate (red) and taurocholate (green) and the two molecules of cholate in the chicken Lb-FABP (yellow). Notice in the figure that the positions of the rings of the molecules in the two alternative NMR structures overlap, to some extent, with one of the cholic acids bound to chicken Lb-FABP, while the more polar ends point in quite different directions. In this context, it should be mentioned that, for human ileal BABP, a stoichiometry of binding of two molecules of glycocholate has been proposed (*25*). Note in Figure 4 that the residues of chicken Lb-FABP involved in ligand binding are rather well conserved or substituted with acceptable alternatives in the four BABPs in the figure with five exceptions: Thr 53 is a Tyr and Arg 55 a Gly in all the BABPs that are listed, Thr 91 is a Val in two and an Ala in the other two sequences, Phe 96 is a Tyr in the four BABPs that are listed, and Gln 100 is a Ser in three of the four BABPs in the figure. Interestingly, one of the five residues that are not conserved, Arg 55, is also one of the most variable among the Lb-FABPs.

Arg 120, strictly conserved in all the Lb-FABPs, the L-FABPs, and the BABPs and identified as the candidate most likely to counterbalance the negative charge of taurocholate in rabbit ileal BABP (*24*), deserves a special comment. In the model of chicken Lb-FABP, the only possible atoms of the ligand that could make a contact with Arg 120 are O3 and O12 of one of the cholate molecules (molecule 130 in our notation) which are, however, ~5 Å from the NH groups of the Arg.

Clearly, the final answer to the question of variability in the mode of bile acid binding to these proteins can only come from experimental data for the two families, but in the meantime, calling the Lb-FABP liver BABPs will probably help to eliminate at least some of the confusion that has surrounded this particular protein family since its discovery.

## ACKNOWLEDGMENT

We thank NASA for the opportunity to grow crystals under microgravity conditions in the International Space Station. We are grateful to Karen Moore and Vicky Johnson of the University of Alabama (Birmingham, AL) for their help in setting up the crystallization experiments and to the staff of Sincrotrone Elettra for assistance during data collection.

## REFERENCES

1. Ockner, R. K., Manning, J. A., Poppenhausen, R. B., and Ho, W. K. (1972) A binding protein for fatty acids in cytosol of intestinal mucosa, liver, myocardium, and other tissues, *Science 177*, 56−58.
2. Banaszak, L., Winter, N., Xu, Z., Bernlohr, D. A., Cowan, S., and Jones, T. A. (1994) Lipid-binding proteins: a family of fatty acid and retinoid transport proteins, *Adv. Protein Chem. 45*, 89−151.
3. Veerkamp, J. H., and Maatman, R. G. H. J. (1995) Cytoplasmic fatty acid-binding proteins: their structure and genes, *Prog. Lipid Res. 34*, 17−52.
4. Glatz, J. F. C., and van der Vusse, G. J. (1996) Cellular fatty acid-binding proteins: their function and physiological significance, *Prog. Lipid Res. 35*, 243−282.

5. Coe, N. R., and Bernlohr, D. A. (1998) Physiological properties and functions of intracellular fatty acid-binding proteins, *Biochim. Biophys. Acta 1391*, 287−306.
6. Schaap, F. G., van der Vusse, G. J., and Glatz, J. F. (2002) Evolution of the family of intracellular lipid binding proteins in vertebrates, *Mol. Cell. Biochem. 239*, 69−77.
7. Sacchettini, J. C., Gordon, J. I., and Banaszak, L. J. (1989) Crystal structure of rat intestinal fatty-acid-binding protein. Refinement and analysis of the *Escherichia coli*-derived protein with bound palmitate, *J. Mol. Biol. 208*, 327−339.
8. Winter, N. S., Gordon, J. I., and Banaszak, L. J. (1990) Characterization of crystalline rat liver fatty acid binding protein produced in *Escherichia coli*, *J. Biol. Chem. 265*, 10955−10958.
9. Thompson, J., Winter, N., Terwey, D., Bratt, J., and Banaszak, L. (1997) The crystal structure of the liver fatty acid-binding protein. A complex with two bound oleates, *J. Biol. Chem. 272*, 7140−7150.
10. Thompson, J., Reese-Wagoner, A., and Banaszak, L. (1999) Liver fatty acid binding protein: species variation and the accommodation of different ligands, *Biochim. Biophys. Acta 1441*, 117−130.
11. Scapin, G., Spadon, P., Pengo, L., Mammi, M., Zanotti, G., and Monaco, H. L. (1988) Chicken liver basic fatty acid-binding protein (pI = 9.0). Purification, crystallization and preliminary X-ray data, *FEBS Lett. 240*, 196−200.
12. Di Pietro, S. M., Dell'Angelica, E. C., Veerkamp, J. H., Sterin-Speziale, N., and Santomé, J. A. (1997) Amino acid sequence, binding properties and evolutionary relationships of the basic liver fatty-acid-binding protein from the catfish *Rhamdia sapo*, *Eur. J. Biochem. 249*, 510−517.
13. Di Pietro, S. M., Veerkamp, J. H., and Santomé, J. A. (1999) Isolation, amino acid sequence determination and binding properties of two fatty-acid-binding proteins from axolotl (*Ambistoma mexicanum*) liver. Evolutionary relationship, *Eur. J. Biochem. 259*, 127−134.
14. Denovan-Wright, E. M., Pierce, M., Sharma, M. K., and Wright, J. M. (2000) cDNA sequence and tissue-specific expression of a basic liver-type fatty acid binding protein in adult zebrafish (*Danio rerio*), *Biochim. Biophys. Acta 1492*, 227−232.
15. Schievano, E., Quarzago, D., Spadon, P., Monaco, H. L., Zanotti, G., and Peggion, E. (1994) Conformational and binding properties of chicken liver basic fatty acid binding protein in solution, *Biopolymers 34*, 879−887.
16. Beringhelli, T., Goldoni, L., Capaldi, S., Bossi, A., Perduca, M., and Monaco, H. L. (2001) Interaction of chicken liver basic fatty acid-binding protein with fatty acids: a $^{13}C$ NMR and fluorescence study, *Biochemistry 40*, 12604−12611.
17. Scapin, G., Spadon, P., Mammi, M., Zanotti, G., and Monaco, H. L. (1990) Crystal structure of chicken liver basic fatty acid-binding protein at 2.7 Å resolution, *Mol. Cell. Biochem. 98*, 95−99.
18. Ceciliani, F., Monaco, H. L., Ronchi, S., Faotto, L., and Spadon, P. (1994) The primary structure of a basic (pI 9.0) fatty acid-binding protein from liver of *Gallus domesticus*, *Comp. Biochem. Physiol. 109B*, 261−271.
19. Walz, D. A., Wider, M. D., Snow, J. W., Dass, C., and Desiderio, D. M. (1988) The complete amino acid sequence of porcine gastrotropin, an ileal protein which stimulates gastric acid and pepsinogen secretion, *J. Biol. Chem. 263*, 14189−14195.
20. Gantz, I., Nothwehr, S. F., Lucey, M., Sacchettini, J. C., DelValle, J., Banaszak, L. J., Naud, M., Gordon, J. I., and Yamada, T. (1989) Gastrotropin: not an enterooxyntin but a member of a family of cytoplasmic hydrophobic ligand binding proteins, *J. Biol. Chem. 264*, 20248−20254.
21. Lin, M. C., Kramer, W., and Wilson, F. A. (1990) Identification of cytosolic and microsomal bile acid-binding proteins in rat ileal enterocytes, *J. Biol. Chem. 265*, 14986−14995.
22. Lücke, C., Zhang, F., Rüterjans, H., Hamilton, J. A., and Sacchettini, J. C. (1996) Flexibility is a likely determinant of binding specificity in the case of ileal lipid binding protein, *Structure 4*, 785−800.
23. Lücke, C., Zhang, F., Hamilton, J. A., Sacchettini, J. C., and Rüterjans, H. (2000) Solution structure of ileal lipid binding protein in complex with glycocholate, *Eur. J. Biochem. 267*, 2929−2938.
24. Kramer, W., Sauber, K., Baringhaus, K.-H., Kurz, M., Stengelin, S., Lange, G., Corsiero, D., Girbig, F., König, W., and Weyland, C. (2001) Identification of the bile acid-binding site of the ileal lipid-binding protein by photoaffinity labeling, *J. Biol. Chem. 276*, 7291−7301.
25. Tochtrop, G. P., Richter, K., Tang, C., Toner, J. J., Covey, D. F., and Cistola, D. P. (2002) Energetics by NMR: site-specific binding in a positively cooperative system, *Proc. Natl. Acad. Sci. U.S.A. 99*, 1847−1852.
26. Kurz, M., Brachvogel, V., Matter, H., Stengelin, S., Thuring, H., and Kramer, W. (2003) Insights into the bile acid transportation system: the human ileal lipid-binding protein-cholyltaurine complex and its comparison with homologous structures, *Proteins: Struct., Funct., Genet. 50*, 312−328.
27. Tochtrop, G. P., Bruns, J. L., Tang, C., Covey, D. F., and Cistola, D. P. (2003) Steroid ring hydroxylation patterns govern cooperativity in human bile acid binding protein, *Biochemistry 42*, 11561−11567.
28. Perduca, M., Bossi, A., Goldoni, L., Monaco, H. L., and Righetti, P. G. (2000) Crystallization of chicken liver (basic) fatty acid binding protein after purification in multicompartment electrolyzers with isolectric membranes, *Electrophoresis 21*, 2316−2320.
29. DeLucas, L. J., Moore, K. M., Long, M. M., Rouleau, R., Bray, T., Crysel, W., and Weise, L. (2002) Protein crystal growth in space, past and future, *J. Cryst. Growth 237−239*, 1646−1650.
30. Leslie, A. G. W. (1992). Recent changes to the MOSFLM package for processing film and image plate data, *Joint CCP4/ESF-EACMB Newsletter on Protein Crystallography 26*, pp 27−33.
31. Collaborative Computational Project Number 4 (1994) The CCP4 suite: programs for protein crystallography, *Acta Crystallogr. D50*, 760−767.
32. Navaza, J. (1994) AMoRe: an automated package for molecular replacement, *Acta Crystallogr. A50*, 157−163.
33. Brunger, A. T., Adams, P. D., Clore, G. M., DeLano, W. L., Gros, P., Grosse-Kunstleve, R. W., et al. (1998) Crystallography and NMR system: a new software suite for macromolecular structure determination, *Acta Crystallogr. D54*, 905−921.
34. Jones, T. A., Zou, J. Y., Cowan, S. W., and Kjeldgaard, M. (1991) Improved methods for the building of protein models in electron density maps and the location of errors in these models, *Acta Crystallogr. A47*, 110−119.
35. Laskowski, R. A., MacArthur, M. W., Moss, D. S., and Thornton, J. M. (1993) PROCHECK: A program to check the stereochemical quality of protein structures, *J. Appl. Crystallogr. 26*, 283−291.
36. Kabsch, W. (1978) A solution for the best rotation to relate two sets of vectors, *Acta Crystallogr. A32*, 922−923.
37. Liang, J., Edelsbrunner, H., and Woodward, C. (1998) Anatomy of protein pockets and cavities: measurement of binding site geometry and implications for ligand design, *Protein Sci. 7*, 1884−1897.
38. Goodford, P. J. (1985) A computational procedure for determining energetically favorable binding sites on biologically important macromolecules, *J. Med. Chem. 28*, 849−857.
39. Kastenholz, M. A., Pastor, M., Cruciani, G., Haaksma, E. E., and Fox, T. (2000) GRID/CPCA: A new computational tool to design selective ligands, *J. Med. Chem. 43*, 3033−3044.
40. Thompson, J. D., Higgins, D. G., and Gibson, T. J. (1994) CLUSTAL W: improving the sensitivity of progressive multiple sequence alignment through sequence weighting, position-specific gap penalties and weight matrix choice, *Nucleic Acids Res. 22*, 4673−4680.
41. Di Pietro, S. M., Córsico, B., Perduca, M., Monaco, H. L., and Santomé, J. A. (2003) Structural and biochemical characterization of toad liver fatty acid-binding protein, *Biochemistry 42*, 8192−8203.


BI0489661